Polymer Chemistry

Accepted Manuscript

ROYAL SOCIETY OF CHEMISTRY

www.rsc.org/polymers

Cite this: DOI: 10.1039/c0xx00000x

www.rsc.org/xxxxxx

ARTICLE TYPE

Molecular design of DBT/DBF hybrid thiophenes π-conjugated systems and comparative study on their electropolymerization and optoelectronic properties: from comonomers to electrochromic polymers

Kaiwen Lin, Shouli Ming, Shijie Zhen, Yao Zhao, Baoyang Lu and Jingkun Xu**

Received (in XXX, XXX) Xth XXXXXXXXX 200X, Accepted Xth XXXXXXXXX 200X
DOI: 10.1039/b000000x

A novel series of comonomers, which comprise dibenzothiophene (DBT) and dibenzofuran (DBF) core symmetrically linked to thiophene and 3-alkylthiophenes at 2 and 8-positions, were designed and electropolymerized to yield the cooresponding electrochromic polymers. Structure-property relationships of comonomers and polymers, including electrochemistry, thermal stability, fluorescence, and electrochromic properties, were systematically explored. In related with core group, alkyl chain group of these polymers had a relatively significant influence on the redox behavior, band gap, neutral state colour, stability, and the electrochromic performance (optical contrast, CE, and switching time) of the system. Furthermore, all the polymer films displayed unique electrochromic characteristic with switching color from yellow to blue. Further kinetic results showed moderate to high optical contrasts (20-70%), high colouration efficiency (typically 170-370 cm^2 C^{-1}), and favorable switching time (0.8-9.4 s). Among them, the electrochromic performance of 3-hexylthiophene-end-capped polymers were superior to those with thiophene/3-methylthiophene as terminal groups. These results demonstrated DBT/DBF-based π-conjugated polymer materials hold promise for display applications and DBT/DBF could be further employed for rational design of excellent electrochromic polymers by matching with other heterocycle units.

1. Introduction

π-Conjugated polymers, due to their mechanical flexibility, environmental stability and ease in tuning their optical and electronic properties *via* structural versatility, have been utilized as electroactive materials for numerous applications, such as organic light emitting diodes (OLEDs), field effect transistors (FETs), sensors, and supercapacitors.[1-3] Especially, π-conjugated polymers as electrochromic materials have been extensively investigated since they exhibited excellent optoelectronic properties including a variety of colours, fast colour-switching ability and high optical contrast as well as their fine-tuning of the band gap (E_g) with minor structural modifications.[4,5] The design and synthesis of novel π-conjugated polymers with specific electrochromic properties have always been one of the primary goals, and served as a challenging pursuit for most chemists working in the area of electrochromic materials.

Among numorous π-conjugated polymer structures, dibenzo-five-membered ring end-capped with heterocycles-based polymers have drawn much attention due to their outstanding electrochromic performances. Previously, fluorene/carbazole-based end-capped with heterocycles-based polymers have been employed as electrochromic materials (their structures are shown in Scheme 1) owing to their excellent redox activity,[6,7] and plentiful colour changes switching between the reduced and oxidized states.[8,9] Besides, all kinds of their derivatives have already been developed and displays a range of unique electrochromic proeprties, such as 3,6-/2,7-carbazoles functionalized at N-position,[10-12] 2,7-fluorenes functionalized at C-9 position.[13-15] For example, Nie and coworkers[16] reported the electropolymerization of 2,7-fluorene end-capped with EDOT units, and the resulting polymer materials exhibited good optical contrast (36% at 625 nm), high colouration efficiency (784 cm^2 C^{-1}) and fast response time (0.5 s at 625 nm). However, despite their intriguing electrochromic performances, the structural cores for dibenzo-five-membered ring end-capped with heterocycles-based polymers are mainly restricted to

School of Pharmacy, Jiangxi Science and Technology Normal University, Nanchang, 330013, China.
Tel: +86-791-88537967; Fax: +86-791-83823320;
Email: lby1258@163.com; xujingkun@tsinghua.org.cn.
†Electronic Supplementary Information (ESI) available: ^1H and ^{13}C NMR spectra of all the intermediates and target compounds; anodic oxidation and chronoamperometric curves, optimized structures; UV-vis spectra of comonomers and TG curves of polymers; switching colours from doped to dedoped states, etc. See DOI: 10.1039/b0000.

fluorenes/carbazoles, and very little is known about their close analogs dibenzofuran and dibenzothiophene, which are also ideal building blocks for π-conjugated systems.[17-18]

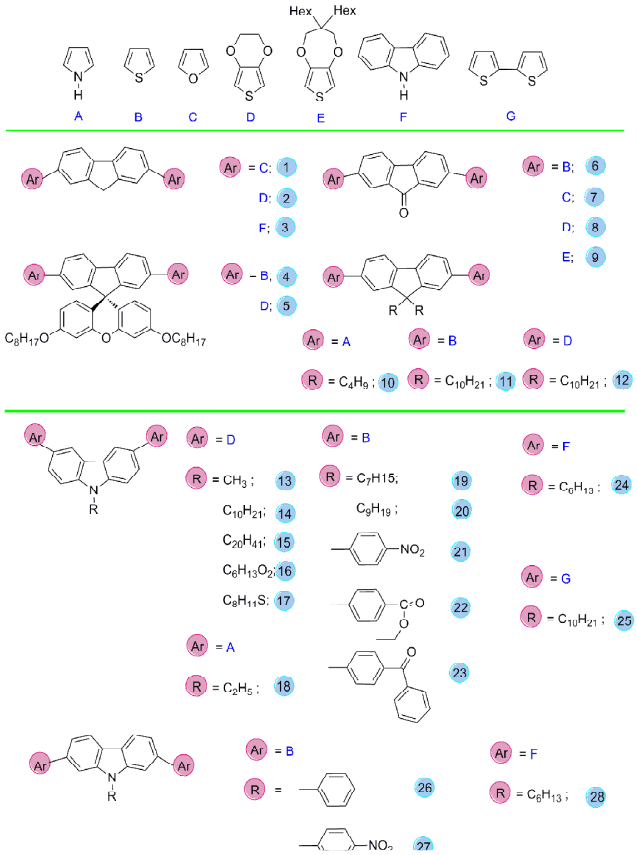

Scheme 1 Chemical structures of dibenzo-five-membered ring end-capped with heterocycles-based polymers as electrochromic materials reported previously.

Similar to carbazole/fluorene, dibenzothiophene (DBT) was previously utilized in constructing new host materials.[19,20] Also, DBT unit was also employed for designing OFET materials with high hole mobility[21,22] due to its p-type nature. Dibenzofuran (DBF) has been used for the biodegradation of biaryl ethers.[23-25] In recent years, DBF was explored as the core structure of high triplet energy host materials for blue PHOLEDs because of its high triplet energy of 3.14 eV.[26-28] Our group recently synthesized two novel blue-light-emitting DBT/DBF end-capped with EDOT monomers (Scheme 2), and the corresponding polymers via their electropolymerization displayed good electrochromic properties.[29] Camurlu et al. [30,31] investigated the synthesis, optical and electrochromic performance of donor–acceptor–donor type monomers: $THSO_2$ and $EDOTSO_2$ (Scheme 2) and used in organic electronic applications. Overall, in comparison with fluorene/carbazole, DBT/DBF-based polymers (as well as their derivatives, Scheme 2) have attracted less attention as electroactive materials. This can be ascribed to the following reasons: (1) These polymers show poor solubility in common organic solvents due to unavailable functionalization at S or O positions, thus hindering their applications in many related fields.[29] (2) As relatively inert or neutral precursors, DBT and DBF require more active reagents and prolonged reaction time.[32] (3) DBT and DBF are relatively expensive compared to fluorenes/carbazoles. Nevertheless, DBT/DBF-based structures could probably lower the high energy barrier of hole injection for fluorene/carbazole-based polymers and extend their applications.[33] Besides, the good rigid planarity of DBT/DBF would improve the stability of target polymers and probably lead to other unexpected properties. Therefore, it is necessary and apparently a challenge to further synthesize and explore DBT/DBF end-capped with heterocycles-based polymers.

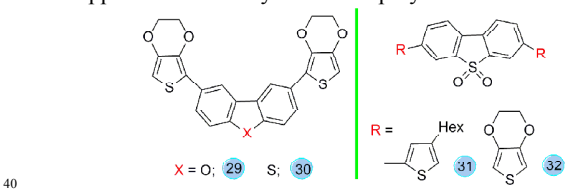

Scheme 2 Reported structures of DBTs/DBF end-capped with thiophenes-based polymers as electrochromic materials previously.

As known, polythiophenes possess many excellent advantages such as ease of synthesis and modification, low band gap, high stability in their oxidized form, good electrical conductivity, etc.[34] As electrochromic materials, many polythiophenes also show various colours in the oxidized and reduced states. Presently, thiophenes-based conjugated polymers have been extensively investigated as active layers in electrochromic applications owing to their unique electrochemical and optical features.[35] Due to these advantages, thiophenes have been always employed for the design of novel π-conjugated systems with outstanding electrochromic performances.

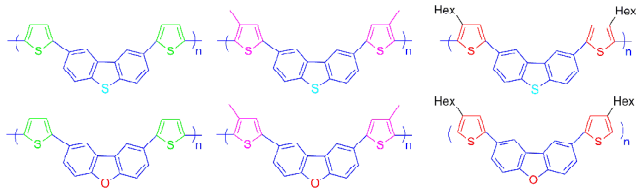

Scheme 3 Designed structures of DBT/DBF end-capped with thiophenes comonomers and their polymers.

It is quite expected that DBT/DBF end-capped with thiophenes-based polymers (Scheme 3) would feature the advantageous combination of DBT/DBF host materials and polythiophenes. Our previous results[29] also demonstrated that the polymer materials from DBF/DBT-EDOT comonomers (29 and 30, Scheme 2) displayed good optoelectronic properties. Herein, a novel series of comonomers, which comprise DBT/DBF core symmetrically linked to thiophene and 3-alkylthiophenes at 2 and 8-positions, were designed and electropolymerized to yield their cooresponding electrochromic polymers. The properties of these comonomers and corresponding polymers including electrochemistry and electrochromics were minutely investigated. Further, the structure–property relationship of these comonomers and polymers were also comparatively discussed.

2. Experimental section

2.1 Chemicals

Bromine, glacial acetic acid, methanol, chloroform, *n*-butyllithium (2.5 mol L^{-1} in hexane), and chlorotributyltin were all purchased from Energy Chemical and used as received. Dibenzothiophene (DBT, 98%; Energy Chemical), dibenzofuran (DBF, 98%; Energy Chemical), thiophene (98%; Energy Chemical), 3-methylthiophene (98%; Energy Chemical), 3-hexylthiophene (98%; Energy Chemical), tetrabutylammonium hexafluorophosphate (Bu_4NPF_6, 98%; Energy Chemical), and tetrakis(triphenylphosphine)palladium(0) ($Pd(PPh_3)_4$, 99%; Energy Chemical) were stored at 4 ºC and used as received. Tetrahydrofuran (THF), dichloromethane (DCM), and acetonitrile (MeCN) were all analytical grade and purchased from Shanghai Vita Chemical Plant and used after reflux distillation. Other chemicals and reagents (analytical grade, >98%) were purchased commercially from Beijing East Longshun Chemical Plant (Beijing, China) and were used without any further treatment.

2.2 Instrumentation

^{1}H NMR and ^{13}C NMR spectra were recorded on a Bruker AV 400 NMR spectrometer at ambient temperature. $CDCl_3$ and DMSO-d_6 were used as the solvent and chemical shifts were recorded in ppm units with tetramethylsilane (TMS) as the internal standard. UV-vis spectra were recorded on Mutispec-1501 Shimadzu Hyper UV-vis spectrophotometer. Infrared spectra were determined with a Bruker Vertex 70 Fourier-transform infrared (FT-IR) spectrometer with samples in KBr pellets. With an F-4500 fluorescence spectrophotometer (Hitachi), fluorescence spectra were determined. Thermogravimetric analysis (TGA) was performed with a Pyris Diamond TG/DTA thermal analyzer (PerkinElmer) under a nitrogen stream from 290 to 1100 K at a heating rate of 10 K min^{-1}.

2.3 Synthesis of comonomers

2.3.1 Synthesis of 2,8-dibromodibenzothiophene[36]

Bromine (3.1 mL, 60.5 mmol) was added dropwise to a mixture of DBT (5.0 g, 27.1 mmol) and chloroform (30.0 mL) at 0 °C. Under nitrogen atmosphere the reaction mixture was stirred 12 h at room temperature. The crude product was filtered off and washed with methanol to isolate 2,8-dibromodibenzothiophene. The product was obtained as a white powder in 85% yield. mp: 218-221 °C; ^{1}H NMR (400 MHz, $CDCl_3$, ppm): δ 7.38 (d, J = 12.2 Hz, 2H), 7.52 (d, J = 7.8 Hz, 2H), 8.05 (d, J = 4.4 Hz, 2H).

2.3.2 Synthesis of 2,8-dibromodibenzofuran[37]

A 250 mL round-bottomed flask containing 8.4 g (50.0 mmol) of dibenzofuran dissolved in 100.0 mL of glacial acetic acid was equipped with an addition funnel. Bromine (5.1 mL, 100.0 mmol) in 30.0 mL of glacial acetic acid was added dropwise *via* the addition funnel to the dibenzofuran under constant stirring. This reaction mixture was stirred at room temperature for 4 h. It was then refluxed for 6 h, and then was cooled to 0 °C. The solid was then collected by filtration and washed with three 100.0 mL portions of water. Recrystallization from 100.0 mL of acetic anhydride obtained 12.2 g (75%) pure 2,8-dibromodibenzofuran as a white solid. mp: 189-192 °C; ^{1}H NMR (400 MHz, $CDCl_3$, ppm): δ 7.44 (d, J = 8.0 Hz, 2H), 7.57 (d, J = 8.6 Hz, 2H), 8.03 (d, J = 3.8 Hz, 2H).

2.3.3 Synthesis of the stannylation of thiophene, 3-methylthiophene and 3-hexylthiophene[38]

A solution of thiophene in dry THF was cooled to -78 °C and blanked by atomsphere (Ar) three times. *n*-BuLi (2.5 mol L^{-1} in hexane) was slowly added dropwise to the solution within 30 min. The mixture was stirred for 1.5 h at -78 °C and then warmed to -40 °C. Chlorotributyltin was added slowly to the solution, after that, the temperature was slowly warmed to room temperature. And the mixture was stirred at room temperature for 12 h under argon atmosphere. The residue was filtered, and then the solvent was removed under reduced pressure by rotary evaporation. The tributylstannane compound was used directly for the Stille coupling reaction without further purification.

Synthesis of 2-tributyl-stannyl-3-methylthiophene and 2-tributyl-stannyl-3-hexylthiophene was carried out in a similar manner to that of thiophene.

2.3.4 Synthesis of 2,8-bis-(thiophen-2-yl)-dibenzothiophene (DBT-Th)

DBT-Th was synthesized *via* Stille coupling reaction as described in Scheme 3. To a mixture solution of 2,8-dibromodibenzothiophene (1.0 g, 2.9 mmol) and tributyl(thiophen-2-yl)stannane (5.4 g, 14.5 mmol) in dry THF and $Pd(PPh_3)_4$ used as the catalyst was also added. The mixture was stirred magnetically at room temperature under nitrogen atmosphere. After 30 min, the mixture was heated to reflux with vigorous stirring for a further 24 h, and then concentrated under reduced pressure. Finally, column chromatography was used to purify the reaction mixture. The product was obtained as a milky white powder in 65% yield. ^{1}H NMR (400 MHz, $CDCl_3$, ppm): δ 7.20 (m, J = 8.2 Hz, 2H), 7.60 (d, J = 8.8 Hz, 2H), 7.75 (d, J = 4.4 Hz, 2H), 7.80 (m, J = 7.6 Hz, 2H), 8.05 (s, 1H), 8.07 (s, 1H), 8.84 (d, J = 4.0 Hz, 2H). ^{13}C NMR (400 MHz, DMSO-d_6, ppm): 143.73, 138.64, 136.07, 131.38, 128.95, 126.18, 125.51, 124.62, 124.14, 119.39.

2.3.5 Synthesis of 2,8-bis-(thiophen-2-yl)-dibenzofuran (DBF-Th)

DBF-Th was synthesized *via* Stille coupling reaction similar to DBT-Th as described in Scheme 3. The product was obtained as a red brown powder in 60% yield. ^{1}H NMR (400 MHz, $CDCl_3$, ppm): δ 7.16 (m, J = 12.6 Hz, 2H), 7.55 (m, J = 15.8 Hz, 4H), 7.72 (d, J = 4.2 Hz, 1H), 7.74 (d, J = 4.8 Hz, 1H), 7.81 (d, J = 4.4 Hz, 1H), 7.84 (d, J = 3.6 Hz, 1H), 8.57 (d, J = 3.4 Hz, 2H). ^{13}C NMR (400 MHz, DMSO-d_6, ppm): 155.90, 143.84, 129.96, 128.98, 126.19, 125.97, 124.69, 124.15, 118.88, 112.76.

2.3.6 Synthesis of 2,8-bis-(4-methyl-thiophen-2-yl)-dibenzothiophene (DBT-3MeTh)

Synthesis of DBT-3MeTh was carried out in a similar manner to that of DBT-Th. Yield: 55%; milky powder. ^{1}H NMR (400 MHz, $CDCl_3$, ppm): δ 2.39 (s, 6H), 7.28 (s, 2H), 7.70 (s, 2H), 7.84 (d, J = 8.2 Hz, 2H), 8.13 (d, J = 7.8 Hz, 2H), 8.90 (s, 2H). ^{13}C NMR (400 MHz, DMSO-d_6, ppm): 142.87, 138.41, 138.02, 135.58, 131.03, 126.25, 124.73, 123.62, 120.78, 118.57, 15.58.

2.3.7 Synthesis of 2,8-bis-(4-methyl-thiophen-2-yl)- dibenzofuran (DBF-3MeTh)

Yield: 55%; red brown powder. ^{1}H NMR (400 MHz, DMSO-d_6, ppm): δ 2.27 (s, 6H), 7.14 (s, 2H), 7.42 (s, 2H), 7.71 (d, J = 7.8 Hz, 2H), 7.78 (d, J = 8.6 Hz, 2H), 8.54 (s, 2H). ^{13}C NMR (400 MHz, DMSO-d_6, ppm): 155.32, 142.94, 138.36, 129.59, 125.85, 125.35, 124.16, 120.54, 118.10, 112.21, 15.56.

2.3.8 Synthesis of 2,8-bis-(4-hexyl-thiophen-2-yl)-dibenzothiophene (DBT-3HexTh)

Yield: 45%; milky powder. ^{1}H NMR (400 MHz, DMSO-d_6, ppm): δ 0.88 (d, J = 8.6 Hz, 6H), 1.33 (s, 12H), 1.65 (d, J = 7.6 Hz, 4H), 2.62 (d, J = 11.8 Hz, 4H), 7.20 (s, 2H), 7.63 (s, 2H), 7.76 (d, J = 8.0 Hz, 2H), 8.04 (d, J = 8.6 Hz, 2H), 8.79 (s, 2H). ^{13}C NMR (400 MHz, DMSO-d_6, ppm): 143.99, 142.80, 137.99, 135.57, 131.09, 125.30, 124.79, 123.61, 120.14, 118.53, 31.07, 30.03, 29.92, 28.42, 22.04, 13.92.

2.3.9 Synthesis of 2,8-bis-(4-hexyl-thiophen-2-yl)-dibenzofuran (DBF-3HexTh)

Yield: 50%; milky powder. ^{1}H NMR (400 MHz, $CDCl_3$, ppm): δ 0.91 (d, J = 8.4 Hz 6H), 1.34 (s, 12H), 1.64 (m, J = 23.6 Hz, 4H), 2.63 (d, J = 11.8 Hz, 4H), 6.89 (s, 2H), 7.22 (s, 2H), 7.54 (d, J = 8.8 Hz, 2H), 7.69 (d, J = 11.2 Hz, 2H), 8.17 (s, 2H). ^{13}C NMR (400 MHz, $CDCl_3$, ppm): 156.06, 144.36, 143.85, 130.03, 125.61, 124.58, 124.46, 119.21, 117.80, 111.94, 31.67, 30.66, 30.41, 29.01, 22.58, 14.07.

2.4 Electrochemistry

All the electrochemical experiments and polymerization of comonomers were performed in a one-compartment cell with the use of Model 263A potentiostat-galvanostat (EG&G Princeton Applied Research) under computer control. For electrochemical tests, the working and counter electrodes were both Pt wires with a diameter of 1 mm, respectively, while the reference electrode was Ag/AgCl. Bu_4NPF_6 (0.1 mol L^{-1}) was used as electrolytes, dissolved in DCM/MeCN (50/50, v/v) which were freshly distilled prior to its use. Polymer films were obtained electrochemically in potentiodynamic regime. After polymerization, the films were washed repeatedly with anhydrous DCM to remove the electrolyte and monomer.

The cyclic voltammetry (CV) and linear sweep voltammetry (LSV) were employed to evaluate the HOMO, LUMO levels and E_g values of comonomers according to the empirical equations as follow:[39-40]

$$\text{HOMO} = -(E_{ox}+4.80)\ \text{eV} \quad (1)$$

$$\text{LUMO} = (\text{HOMO}+E_{g,opt})\ \text{eV} \quad (2)$$

where E_{ox} and $E_{g,opt}$ are the onset oxidation potential and the optical bandgap of compounds, respectively.

2.5 Electrochromic experiments

Spectroelectrochemistry and kinetic studies were recorded on a Specord 200 plus (Analytik Jena) spectrophotometer and the potentials were controlled using Versa STAT 3 (Princeton Applied Research). The spectroelectrochemical cell consisted of a quartz cell, an Ag/AgCl electrode, a Pt wire, and an indium tin oxide (ITO) coated glass as the transparent working electrode. All measurements were carried out in MeCN containing 0.1 mol L^{-1} Bu_4NPF_6 as the supporting electrolyte.

The optical density (ΔOD) at the specific wavelength (λ) was determined by ΔT% values of electrochemically oxidized and reduced polymer films, using the following equation:[41]

$$\Delta OD = \log(T_{ox}/T_{red}) \quad (3)$$

The colouration efficiency (CE) is defined as the relation between the injected/ejected charge as a function of electrode area (Q_d) and the change in optical density (ΔOD) at the specific wavelength (λ) of the sample as illustrated by the following equation:[42]

$$CE = \Delta OD/Q_d \quad (4)$$

3. Results and Discussion

3.1 Monomer Synthesis

The molecular design and synthesis of new comonomers is the most effective way in order to fine-tune the electrochemical and electrochromic properties of conjugated polymers. Scheme 4 shows the synthetic routes for DBT/DBF end-capped with thiophenes comonomers; the detailed synthesis procedures are described in the experimental section. In this context, the key comonomers were synthesized from DBT/DBF by a three-step procedure, including bromination of DBT/DBF, synthesis of 2-tributyl-stannyl-thiophene/2-tributyl-stannyl-3-methylthiophene /2-tributyl-stannyl-3-hexylthiophene, and then the Stille coupling with satisfied yields. The resulting DBT/DBF-based polymers, namely PBDT-Th, PDBT-3MeTh, PDBT-3HexTh, PBDF-Th, PDBF-3MeTh, and PDBF-3HexTh, were obtained via electrochemical polymerization. During the synthetic procedure, we had to adopt fast column chromatography in the purification of these comonomers and store them in refrigerator before use (4 °C). To the best of our knowledge, these comonomers were synthesized and investigated for the first time. ^{1}H and ^{13}C NMR spectra of some intermediates and target compounds are displayed in Fig. S1-S14.

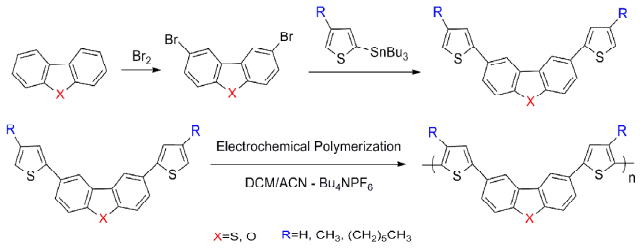

Scheme 4 Synthetic routes of DBT/DBF end-capped with thiophenes comonomers and their electropolymerization.

3.2 Electrochemical polymerization of comonomers

The electropolymerization performances of these comonomers (0.01 mol L^{-1}) were examined in a DCM/MeCN (50/50, v/v) solution containing 0.1 mol L^{-1} Bu_4NPF_6 as the electrolyte. All the comonomers can easily dissolve in DCM, while partly dissolve in MeCN. Simultaneously, the polymers became rough, discontinuous and heterogeneous easily when electropolymerized in DCM. Therefore, a mixture of DCM and MeCN (50/50, v/v) was chosen as the solvent system to obtain the polymer film on ITO coated glass slide. From their anodic oxidation curves (Fig. S15), the onset oxidation potentials (E_{onset}) were initiated between

1.00 and 1.20 V (Table 1). As anticipated, the increase in the chain length of alkyl chain attached to thiophene unit increased the electron-donating ability and thus, the onset oxidation potential of 3-hexylthiophene-substituted comonomers lowered in comparison with 3-thiophene/methylthiophene-end-capped comonomers.[43] In addition, the onset oxidation potentials of DBF-based comonomers were higher than those of DBT-based comonomers while coupling with the same terminal groups. This is an expected result because the electron-donating ability of the oxygen atom is weaker than the sulfur atom which lowers the electron density of the comonomer systems. Furthermore, the oxidation potentials of these comonomers are significantly lower than those of thiophenes and DBT/DBF due to the elongation of the conjugated systems. However, these calues are all higher than DBT-EDOT and DBF-EDOT (0.91 V and 0.95 V *vs.* Ag/AgCl),[29] mainly owing to the strong electron-donating EDOT as the terminal group.

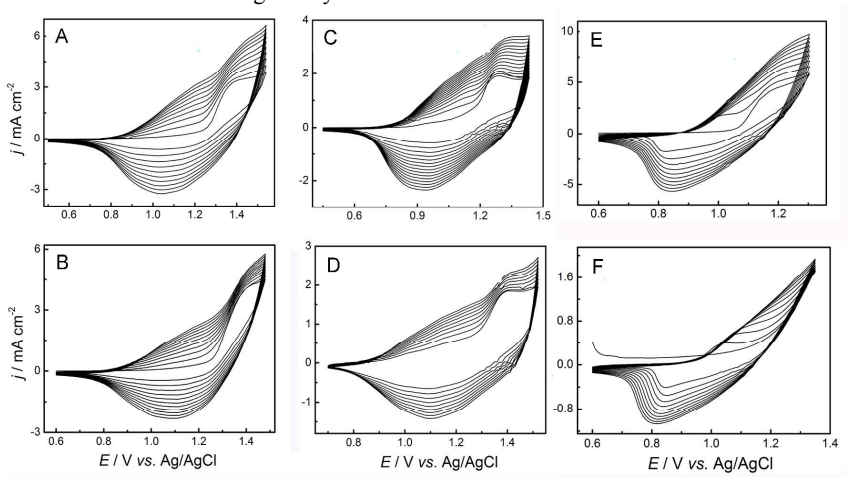

Fig. 1 Cyclic voltammograms of 0.01 mol L^{-1} DBT-Th (A), DBF-Th (B), DBT-3MeTh (C), DBF-3MeTh (D), DBT-3HexTh (E) and DBF-3HexTh (F) in DCM/MeCN-Bu_4NPF_6 (0.1 mol L^{-1}). Potential scan rate: 100 mV S^{-1}.

Cyclic voltammetry (CV) studies reveal the reversibility of the electron transfer for comonomers and polymers. Fig. 1 shows the cyclic voltammograms (CVs) corresponding to the potentiodynamic electropolymerization of the comonomers. All these comonomers showed characteristic features of typical conducting polymers during potentiodynamic synthesis, also in good agreement with thiophene and 3-alkylthiophenes. Typically, the current densities on the reverse scan were higher than that on the forward scan. The formation of this first loop can be explained as characteristic of the nucleation process.[44] Comonomers with 3-hexylthiophene as the terminal group revealed lower redox potentials than other comonomers probably owing to the strong electron-donating effect of hexyl group. During polymerization, visual inspection also revealed the formation of compact and homogeneous polymer films on the electrode surface. The increase of anodic and cathodic peak current densities in the CVs implied an increasing amount of polymer film on the electrode surface.[45] Furthermore, the broad redox peaks of the polymer might be ascribed to the wide distribution of polymer chain length or the conversion of conductive species on the polymer main chain from the neutral to the metallic state.[46]

The HOMO energy levels of these comonomers were calculated from linear sweep voltammetry from the intersection between base line and tangent drawn to the increasing current line. LUMO levels were estimated from the band gap values obtained from UV-vis spectra, and the values were given in Table 1. The HOMO levels for DBT-based comonomers lie higher than DBF-based ones, whereas LUMO levels for DBF-based comonomers lower.

Table 1. Electrochemical and optical data for comonomers

Sample	$\lambda_{max,1}$ (nm)	$\lambda_{max,2}$ (nm)	$\lambda_{max,3}$ (nm)	HOMO (eV)	LUMO (eV)	$E_{ox,onset}$ (V)	$E_{g,opt}$ (eV)
DBT-Th	261	271	307	-5.92	-2.37	1.12	3.55
DBF-Th	253	263	301	-6.01	-2.74	1.21	3.27
DBT-3MeTh	261	271	310	-5.94	-2.44	1.11	3.50
DBF-3MeTh	253	263	310	-6.03	-2.81	1.23	3.22
DBT-3HexTh	261	272	312	-5.83	-2.30	1.03	3.53
DBF-3HexTh	254	263	305	-5.91	-2.52	1.11	3.39

3.3 Optimization of electrical conditions and preparation of polymers

Potentiostatic electrolysis was employed to prepare the polymer films for characterization. To optimize the applied potentials for polymerization, a set of current transients during the electropolymerization at different applied potentials were recorded, as shown in Fig. S16. Typically, at applied potentials below the onset oxidation potential, no polymer film was found on the electrode. Once the applied potential reached the threshold value, all the electrosynthetic current densities initially experienced a sharp increased and then a slow decreased and finally kept constant as a result of uniform deposition of the polymer film on the electrode surface. However, at relatively high potentials, the surfaces of the polymer films became discontinuous and heterogeneous. This phenomenon was mainly due to the significant overoxidation at higher potentials, which led to poor quality films.[47] Therefore, the optimized polymerization potentials were optimized to be 1.45 V for DBT-Th, 1.40 V for DBF-Th, 1.40 V for DBT-3MeT, 1.45 V for DBF-3MeTh, 1.20 V for DBT-3HexTh, and 1.30 V for DBF-3HexTh, respectively. Also, visual inspection demonstrated that all these polymer films with smooth, homogeneous, and continuous surfaces were formed at applied potentials, as predicted from their *I-t* curves, and they displayed good adherence against the electrode.

3.4 Electrochemistry of the polymers

The electrochemical behavior of the polymer-modified Pt electrodes was studied by cyclic voltammetry in the monomer-free electrolyte to test their electroactivity and stability and the results are shown in Fig. 2.

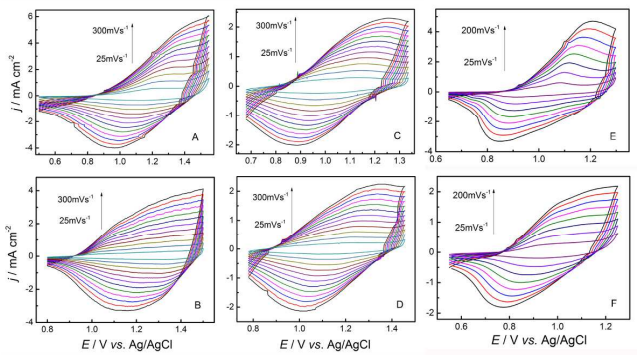

Fig. 2 Cyclic voltammograms of PDBT-Th (A), PDBF-Th (B), PDBT-3MeTh (C), PDBF-3MeTh (D) DBT-3HexTh (E) and DBF-3HexTh (F) modified Pt electrodes in monomer-free DCM/MeCN-Bu_4NPF_6 (0.10 mol L^{-1}).

The CVs of all the polymers under different potential scan rates illustrated broad anodic and cathodic peaks like polythiophenes.[48] In addition, CVs of all polymers in monomer-free electrolytes demonstrated an obvious hysteresis, *i.e.*, an obvious potential drift between the anodic and cathodic peak potentials.[49-50] The potential shift of redox peaks among CVs curves for conducting polymers is hardly explained by conventional kinetic limitations such as ion diffusion or interfacial charge transfer processes. The main reasons that account for this phenomenon are usually as follows: slow heterogeneous electron transfer, local rearrangement of polymer chains, slow mutual transformation of various electronic species, and electronic charging of interfacial exchange corresponding to the metal/polymer and polymer/solution interfaces.[51]

All peak current densities were well proportional to the potential scanning rate (Fig. 3 and Table 2), indicating that the redox process was non-diffusional and electroactive materials were well-adhered to the working electrode.[52] Importantly, the calculated $j_{p,a}/j_{p,c}$ (anodic and cathodic ratio of peak current, oxidation and reduction ratio of charges, respectively) of DBF-based polymers were closer to 1.0, better than those of DBT-based polymers, indicating their better redox reversibility.

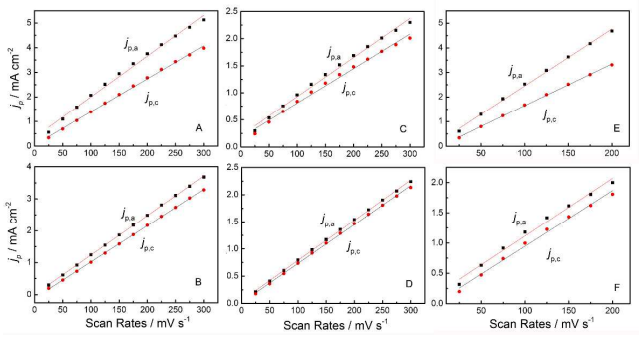

Fig. 3 Plots of redox peak current densities *vs*. potential scan rates. j_p is the peak current density, and $j_{p,a}$ and $j_{p,c}$ denote the anodic and cathodic peak current densities, respectively.

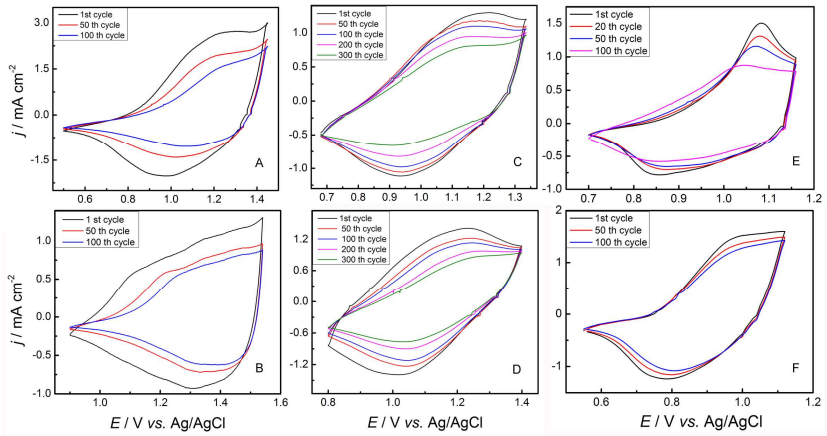

Fig. 4 Long-term CVs of PDBT-Th (A), PDBF-Th (B), PDBT-3MeTh (C), PDBF-3MeTh (D) DBT-3HexTh (E) and DBF-3HexTh (F) in monomer-free DCM/MeCN-Bu_4NPF_6 (0.10 mol L^{-1}) upon repeated cycling at the scan rate of 150 mV s^{-1}.

Cite this: DOI: 10.1039/c0xx00000x

www.rsc.org/xxxxxx

ARTICLE TYPE

As we all know, the good stability of conducting polymers is a key property for their applications in advanced technological applications.[53] For example, the long-term stability upon switching and/or cycling plays a key role in the electrochromic performance of electronic devices and smart windows. Therefore, the long-term stability of these polymers were investigated in monomer-free electrolyte solution by applying potential pulses at the potential scan rate of 150 mV s^{-1}, as shown in Fig. 4. From Fig. 4 and Table 2, all these polymers experienced an obvious degragation over 10% just after 100 cycles. In particular, the exchange charge of thiophene-end-capped polymers remained less than 50%, indicating their insufficient stability against cycling, even inferior to polythiophene.[54] With the introduction of alkyl groups on thiophene units, the resulting polymers displayed better stability, comparable to PDBT/PDBF-EDOT (83.8% and 88.5% after 100 cycles).[29] Typically, 84.2% for PDBT-3HexTh and 88.0% for PDBF-3HexTh of their electrochemical activity was maintained after 100 cycles, respectively (Table 2).

3.5 Structural characterization

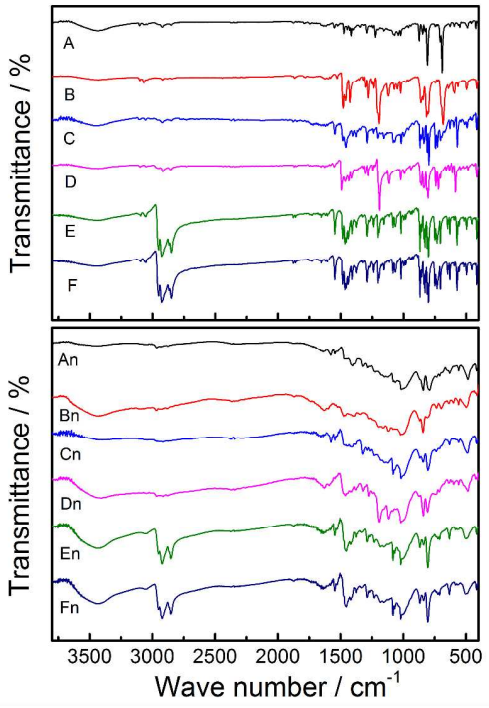

Fig. 5 FT-IR spectra of the comonomers and their corresponding polymers: DBT-Th (A), DBF-Th (B), DBT-3MeTh (C), DBF-3MeTh (D), DBT-3HexTh (E) , DBF-3HexTh (F), PDBT-Th (An), PDBF-Th (Bn), PDBT-3MeTh (Cn), PDBF-3MeTh (Dn), PDBT-3HexTh (En), and PDBF-3HexTh (Fn).

FT-IR spectra of the comonomers and their corresponding polymers were recorded to elucidate their structure and interpret the polymerization mechanism. As can be seen from Fig. 5, the absorption peaks in the spectra of the doped polymers were obviously broadened in comparison with those of comonomers, similar to those of other conjugated polymers with similar structures reported previously.[55-57] This phenomenon was probably due to the fact that the resulting product was composed of oligomers/polymers with wide chain dispersity. For all polymers, the bands due to C_{α}-H stretching of thiophenes at approximately 3106 cm^{-1} and C_{β}-H stretching of thiophenes at 3047 cm^{-1} in the monomer spectra were nearly absent or weakened, while those in the 3000-2800 cm^{-1} region remained. This indicated the occurrence of electropolymerization at the thiophene rings. In the fingerprint region, the emergence of the characteristic peaks at approximately 861-876 cm^{-1} could be attributed to the out-of-plane bending vibration of adjacent C-H in the thiophene groups. This confirmed that the polymerization occured primarily at α-positions of thiophenes, namely, $C_{(2)}$ and $C_{(5)}$ positions, in good agreement with previous reports.[56] Obviously, 3-hexylthiophene-substituted comonomers and polymers demonstrated obvious characteristic peaks at 2940-2840 cm^{-1} which were attributable to C-H stretching of $-CH_2$ and $-CH_3$. In addition, the new sharp peaks appearing at around 839 cm^{-1} and 558 cm^{-1} indicated the presence of doping anions PF_6^-. Further details of the band assignments for comonomers and polymers are given in Table S2.

3.6 Solubility, UV-vis and fluorescence spectra of comonomers and their corresponding polymers

Although comonomers show good solubility in conventional organic solvents, as-prepared films were partly soluble in common organic solvents such as DCM, acetone, diethyl ether, *etc.* The poor solubility of the polymers is due to their longer polymer chain sequences after polymerization. And out of our expectation, the increase in the alkyl chain length attached to the thiophene units had little effect on solubility.

From the UV-vis spectra of comonomers examined in MeCN (Fig. S17), all the comonomers showed similar absorption due to their close structures, and exhibited characteristic π-π* transition peaks in the range of 250~310 nm (Table 1). The changes in the alkyl chain length on thiophene units exhibited no significant shifts in UV-vis spectra. Meanwhile, the absorption peaks of DBT-based comonomers revealed red shift compared with DBF-based comonomers while their overall absorption tailed off to 350-355 nm in comparison with those DBF-based comonomers (366-385 nm). The optical band gaps (E_g^{opt}) were calculated from the onset of the optical absorption spectra (λ_{onset}), as shown in Table 1.

The fluorescence emission spectra of comonomers and dedoped polymers were determined in MeCN (Fig. 6). In accordance with the UV-vis spectral results, the emission spectra of comonomers displayed no obvious shifts with the variation of structural changes (emission peaks from 395 to 410 nm, Fig. 6). However, obvious red shifts could be observed between

comonomers and the soluble polymers, primarily due to the elongation of delocalized π-electron chain sequence of the polymer.

Table 2. Optical and electrochemical properties of the polymers

Polymers	Electrochemistry and linear fitting				Redox stability		Absorption		
	$E_{ox,peak}$ (V)	$E_{red,peak}$ (V)	R^2_{an}	R^2_{cat}	100th	300th	λ_{onset} (nm)	λ_{max} (nm)	$E_{g,opt}$
PDBT-Th	1.39	1.04	0.997	0.999	48.8%	--	490	410	2.53
PDBF-Th	1.40	1.10	0.999	0.999	47.2%	--	515	392	2.41
PDBT-3MeTh	1.28	0.93	0.996	0.996	87.1%	60.2%	472	392	2.63
PDBF-3MeTh	1.39	1.10	0.999	0.999	72.5%	42.8%	504	402	2.46
PDBT-3HexTh	1.19	0.84	0.998	0.999	84.2%	--	429	360	2.89
PDBF-3HexTh	--	0.81	0.995	0.996	88.0%	--	451	330	2.75

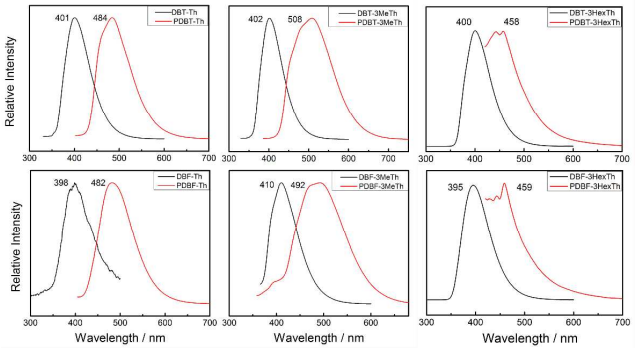

Fig. 6 Fluorescence emission spectra of the comonomers and their corresponding polymers in MeCN.

3.7 Thermal Analysis

Thermal degradation behavior of conducting polymers is very important for their potential applications. To investigate the thermal stability of the polymers, thermogravimetric analytical experiments were performed under a nitrogen stream at a heating rate of 10 K min^{-1}, as shown in Fig. S18. The curves of thermal degradation can be divided roughly into three sections, and it can be clearly observed that the polymer initially underwent a small weight decrease about 3.4~6.5% for all the polymers at relatively low temperature (from 290 K to 400 K), which may be attributed to moisture evaporation trapped in the polymer according to many authors.[58] With the gradual increasing of the temperature, a more prominent weight loss step was clearly found at 400 K < T < 1000 K for thiophene or 3-methylthiophene-end-capped polymers and 400 K < T < 800 K for 3-hexylthiophene-end-capped polymer films. Such a prominent weight loss was closely related to the oxidizing decomposition of the skeletal backbone chain structure. Among them, 3-hexylthiophene-end-capped polymers were easily to crack and thiophene or 3-methylthiophene-end-capped polymers needed higher temperature to decompose the skeletal backbone chain structure. The following degradation after 1000 K or 800 K was probably caused by the overflow of segments decomposed from polymers mentioned previously. When the temperature increased up to about 1100 K, and the residue for all the polymers was more than 55%. Overall, these results indicated outstanding thermal stability of all the polymer films were obtained, and clearly better than its EDOT analogs,[29] which will benefit for the eletrochromic application of these conducting polymers.[59]

3.8 Morphology

Scanning electron microscopy (SEM) is a useful method to investigate the surface morphology of the polymer film for analyzing its constituent and texture. Therefore, the surface of both the doped and dedoped polymer films deposited electrochemically on the ITO electrode was observed by scanning electron microscopy (Fig. S19). Macroscopically, all the polymer films exhibited smooth and compact morphology at both doped and dedoped states. At the magnification of 2000×, all of the polymer films still displayed smooth surface but with significant defects. A lot of holes with different diameters could be observed from the images. This is a common morphology often observed for electrosynthesized conducting polymer films, especially at high polymerization rates. Interestingly, no obvious difference was observed between the surface morphology of all the doped and dedoped polymer films, indicating that the migration of counter ions out of/into the polymer films during the doping/dedoping processes did not destroy their original morphology.

3.9 Spectroelectrochemistry

In order to probe the electronic structure of the polymers and examine the nature of electrochromism in the electrochromic polymers, spectroelectrochemical analyses were performed.[60] Therefore, the polymer films on ITO were elaborated by recording the changes in the absorption spectra under a variety of voltage pulses after neutralization at 0 V.

The electronic absorption spectra of the films in the neutral form illustrated similar absorption band at around 410 nm, 392 nm, 392 nm, and 402 nm, for PDBT-Th, PDBF-Th, PDBT-3MeTh, and PDBF-3MeTh, whereas PDBT-3HexTh and PDBF-3HexTh, differed from thiophene/3-methylthiophene-substituted polymers, showed absorption band at around 360 nm and 330 nm corresponding to the π-π* transitions. This blue shift might be attributed to the steric hindrance effect of hexyl group, which decreased the degree of polymerization and then the length of the conjugated chain.

Upon oxidation, the intensity of the absorption bands began to decrease simultaneously with the increase in the visible and near-IR region (Fig. 7), representing the formation of polaronic and bipolaronic bands.[61] Polaronic absorption at 560 nm emerged with oxidation was tailed into the visible region, which contributed to the colour of the polymer. Take PDBT-Th for example, as the valence-conduction band at 410 nm diminished, a new band started to intensify at about 540 nm in the potential range of 0.60-1.00 V. Upon further oxidation, beyond 1.00 V, this band underwent a blue shift to 530 nm which was accompanied with a new broad band around 1020 nm. All spectra recorded

during potential cycling between 0.60 and 1.30 V passed through a clear isosbestic points at around 450 nm, indicating that the polymer films were being interconverted between its neutral and oxidized states. The changes in the electronic absorption spectra of PDBT-Th films were also accompanied by a colour change from yellow to dark blue, indicating that PDBT-Th film illustrated electrochromic behavior. The spectroelectrochemical changes recorded for other polymer films, were alomost same to those of PDBT-Th, in terms of the formation of two absorption bands (Table 3), indicating the formation of polaronic and bipolaronic.

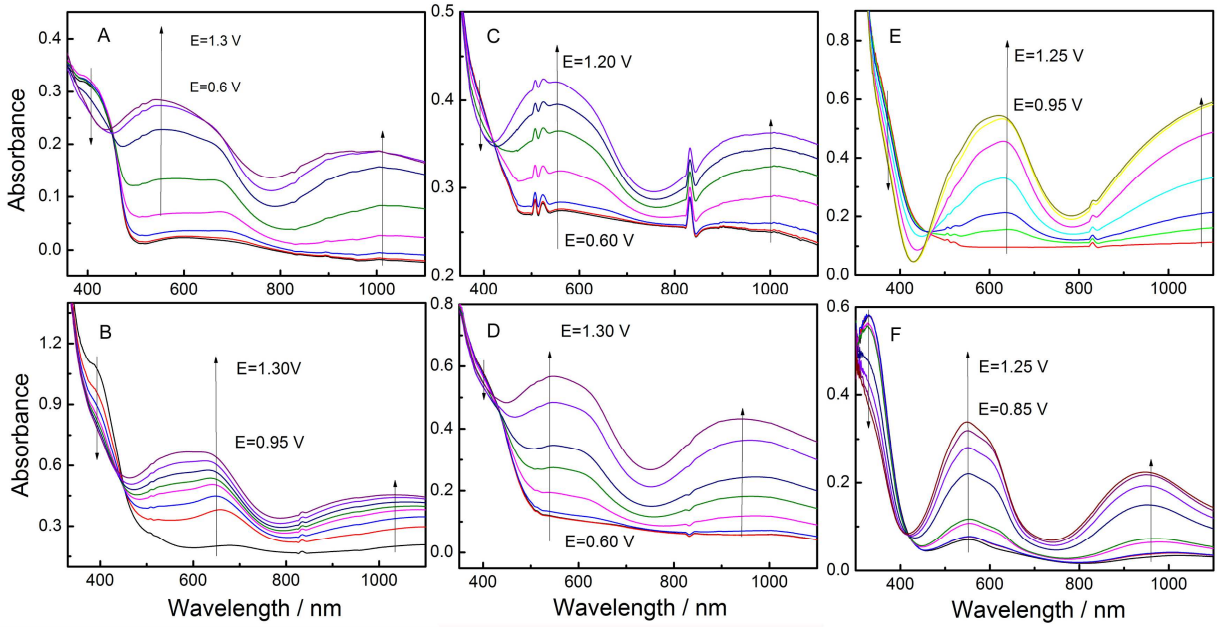

Fig. 7 Spectroelectrochemistry for PDBT-Th (A), PDBF-Th (B), PDBT-3MeTh (C), PDBF-3MeTh (D) PDBT-3HexTh (E), and PDBF-3HexTh (F) on the ITO coated glass in MeCN-Bu_4NPF_6 (0.1 mol L^{-1}) between the potentials indicated (ΔE = 0.05 V for B, E and F, ΔE = 0.10 V for A, C and D).

E_g values of the polymer films deposited on ITO electrodes *via* constant potential electrolysis determined from the commencement of low energy end of π-π* transitions, utilizing spectroelectrochemical data and were calculated to be in the range of 2.41~2.89 eV according to the Planck equation (E_g=1241/λ_{onset}, Table 2). The longer wavelength is the absorption, the higher conjugation length is the polymer.[31] Therefore, compared with comonomers, the red shifts for polymers were due to their longer chain length. These spectral results confirmed the occurrence of electrochemical polymerisation. In addition, it is found that with same terminal thiophene groups, DBT-based comonomers and polymers displayed higer E_g values in comparison with DBF-based comonomers and polymers.

To determine the colour change, the CIE 1976 (L*, a*, b*) colour space and photographs were determined in which L* is the parameter of the lightness, a* is the red-green balance and b* is yellow-blue balance (−a* and +a* correspond to green and red and −b* and +b* correspond to blue and yellow, respectively).[62-63] The details colourimetric data with a D65 illuminant as detailed for synthesized polymers are given in Table S3. Overall, fully oxidized states polymer films on one piece of ITO-coated glass were easily to obtain, and all polymers illustrated similar colours (dark blue), which were similar to 1,[64] 2,[16] 9,[65] 20,[66] 22,[67] and 27[68] in Scheme 1. With the polymer film thickness increasing, more saturated blue colours was achieved and even seemed to be black. In addition, all the neutral state colours ranged from vibrant yellows similar to PDBT-Th to colours bordering on or falling into the yellow-green region such as the case for PDBT-3MeTh, while PDBT-3HexTh and PDBF-3HexTh were transparent gray, differed from other four polymers as well as their analogues displayed in Scheme 1 and Scheme 2.

3.10 Electrochromic properties

Optical switching studies of the polymer films were carried out using a square wave potential step method coupled with optical spectroscopy (chronoabsorptometry) in monomer-free MeCN-Bu_4NPF_6 (0.10 mol L^{-1}) solution. The electrochromic parameters including optical contrast ratio (ΔT%) and response time were investigated by increment and decrement in the transmittance with respect to time at specific absorption wavelengths. The potentials were alternated between the reduced and oxidized states with a residence time of 10 s. Electrochromic parameters of all the polymer films were summarized in Fig. 8 and Table 3.

All the polymers displayed moderate to high optical contrasts at different wavelengths and decent colouration efficiency (*CE*) values (at 95% of the full contrast). As can be seen in Fig. 8, DBT-based polymers displayed ideal optical contrast ratio in the range of 20-70% at different wavelengths. In particular, PDBT-3HexTh reached the highest ΔT% (69% at 625 nm). This result was far ahead among its heteroanalogues which displayed in Scheme 1 and Scheme 2 (Table S1). Meanwhile, relatively high *CE* values (372 cm^2 C^{-1} at 550 nm) was calculated for PDBF-3HexTh. However, these polymers switched slowly between their neutral and oxidized states. PDBT-Th and PDBT-3HexTh revealed unsatisfied switching times of 9.4 s at 410 nm and 9.4 s at 360 nm to achieve 95% of their optical contrasts for the doping process. Meanwhile, these dedoping

process revealed impressive switching times of 0.8 s and 0.8 s. All these six polymers switched more rapidly in the neutral state than in the oxidized state. Simultaneously, note here that the switching speed usually depends on several factors such as the ionic conductivity of the electrolyte, accessibility of the ions to the electroactive sites (ion diffusion in thin films), magnitude of the applied potential, film thickness, and morphology of the thin film.[69]

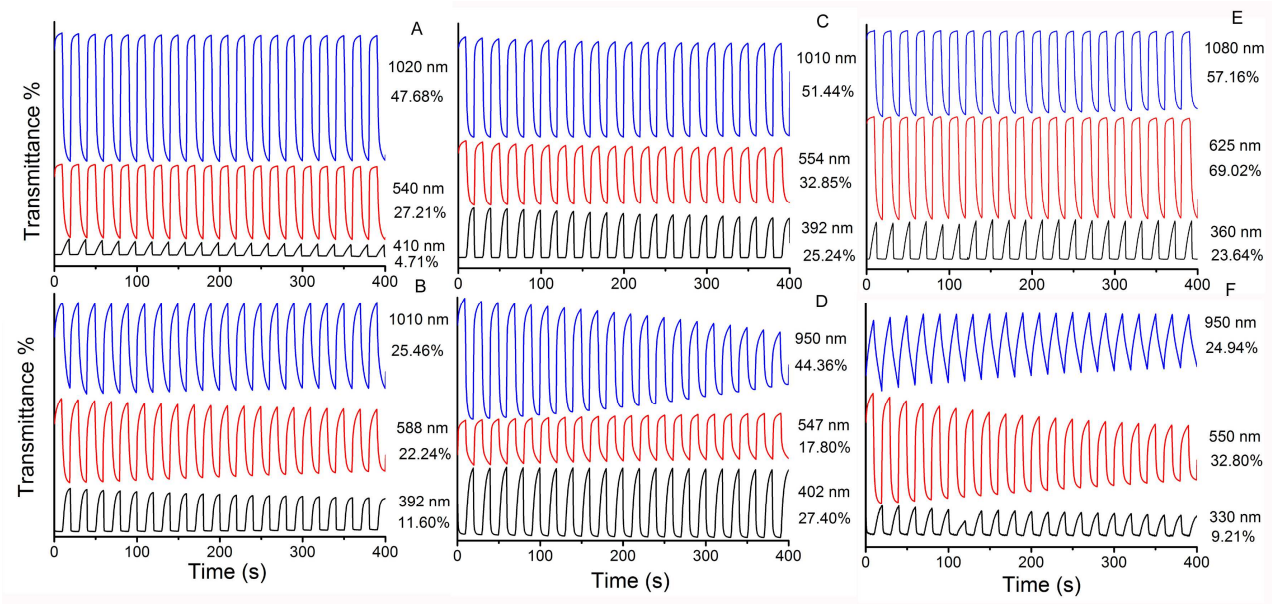

Fig. 8 Electrochromic switching responses: optical absorbance change monitored for PDBT-Th (A), PDBF-Th (B), PDBT-3MeTh (C), PDBF-3MeTh (D) PDBT-3HexTh (E) and PDBF-3HexTh (F) in monomer-free MeCN-Bu_4NPF_6 (0.1 mol L^{-1}). Switching time: 10 s.

By considering all the above data concerning electrochromic properties, it can be clearly observed that all the polymer films displayed unique electrochromic characteristic with switching color from yellow to blue. Further kinetic results showed moderate to high optical contrasts (20-70%), high colouration efficiency (typically 170-370 cm^2 C^{-1}), and favorable switching time (0.8-9.4 s). Among them, the electrochromic performance of 3-hexylthiophene-end-capped polymers were superior to those with thiophene/3-methylthiophene as terminal groups. We ascribed this situation to the following two reasons: (1) By employing 3-hexylthiophene as the terminal groups, the polymer exhibited better optoelectronic properties than those of thiophene/3-methylthiophene as ending groups, which was mainly attributed to the electron-donating effect of longer alkyl chain hexyl group; (2) The onset oxidation and polymerization potential were successively decreased in comparison with other comonomers, leading to obtain the inform electrodeposition of polymer films with improved quality at relatively low potentials.

Table 3. Electrochromic parameters of the polymers at different wavelengths

Sample	Wavelength (nm)	ΔT	Response time (s)		*CE* (cm^2 C^{-1})
			Oxidation	Reduction	
PDBT-Th	410	4.71%	9.4	0.8	22
	540	27.21%	6.8	2.4	72
	1020	47.68%	5.8	2.6	104
PDBF-Th	392	11.60%	7.0	1.0	262
	588	22.24%	5.6	7.4	215
	1010	25.46%	7.2	7.2	197
PDBT-3MeTh	392	25.24%	7.8	1.0	168
	554	32.85%	6.0	5.0	124
	1010	51.44%	4.8	4.2	174
PDBF-3MeTh	402	27.40%	8.2	2.2	184
	547	17.80%	7.6	5.8	359
	950	44.36%	4.6	5.8	165
PDBT-3HexTh	360	23.64%	9.4	0.8	330
	625	69.02%	7.2	1.8	304
	1080	57.16%	6.0	1.6	241
PDBF-3HexTh	330	9.21%	9.0	2.6	214
	550	32.80%	4.6	6.6	372
	950	24.94%	9.2	9.0	160

4. Conclusions

In summary, the design, synthesis, and characterization of a series of thiophenes-end-capped DBT/DBF conjugated systems, were described, and the optoeletronic and electrochromism of both the comonomers and polymers were minutely explored. Also, the effect of the core group (DBT/DBF) and terminal thiophene units (Th, 3MeTh, and 3HexTh) on the structure-property relationships was discussed. In related with core group, alkyl chain group of these polymers had a relatively significant influence on the redox behavior, band gap, neutral state colour, stability, and the electrochromic performance (optical contrast, *CE*, and switching time) of the system. It was noted that all these polymer films prepared *via* electrochemical process onto transparent ITO/glass surface led to impressive colour persistent electrochromic material at different redox states, which illustrated high *CE*, high transmittance. Based on these preliminary results, these novel polymer materials provide more plentiful electrochromic colours and hold promise for display applications. Moreover, DBT/DBF could be further employed for rational design of excellent electrochromic polymers by matching with other heterocycle units.

Acknowledgement

We are grateful to the National Natural Science Foundation of China (grant number: 51303073, 51463008), Ganpo Outstanding Talents 555 projects (2013), the Training Plan for the Main Subject of Academic Leaders of Jiangxi Province (2011), the Science and Technology Landing Plan of Universities in Jiangxi province (KJLD12081), the Natural Science Foundation of Jiangxi Province (grant number: 20122BAB216011, 20142BAB206028, 20142BAB216029), and Provincial Projects for Postgraduate Innovation in Jiangxi (YC2014-S431, YC2014-S441) for their financial support of this work.

References

1 Ozyurt, F.; Gunbas, E. G.; Durmus, A.; Toppare, L. *Org. Electron.* **2008**, 9, 296–302.
2 Kaya, I.; Yildirim, M.; Aydin, A. *Org. Electron.* **2011**, 12, 210–218.
3 Wang, C. L.; Dong, H. L.; Hu, W. P.; Liu, Y. Q.; Zhu, D. B. *Chem. Rev.* **2012**, 112, 2208–2267.
4 Yigitsoy, B.; Karim, S. M. A.; Balan, B.; Baran, D.; Toppare, L. *Synth. Met.* **2010**, 160, 2534–2539.
5 Wen, L.; Amb, C. M.; Rasmussen, S. C. *J. Org. Chem.* **2008**, 73, 8529–8536.
6 Wu, F. I.; Shih, P. I.; Shu, C. F.; Tung, Y. L.; Chi, Y. *Macromolecules* **2005**, 38, 9028–9036.
7 Yang, Y.; Pei, Q. *J. Appl. Phys.* **1997**, 81, 3294–3298.
8 Morin, J. F.; Leclerc, M.; Ades, D.; Siove, A. *Macromol. Rapid Commun.* **2005,** 26, 761–778.
9 Bloudin, N.; Michaud, A.; Leclerc, M. *Adv. Mater.* **2007**, 19, 2295–2300.
10 Koyuncu, S.; Usluer, O.; Can, M.; Demic, S.; Icli, S.; Sariciftci, N. S. *J. Mater. Chem.* **2011**, 21, 2684–2693.
11 Koyuncu, F. B.; Koyuncu, S.; Ozdemir, E. *Org. Electron.* **2011**, 12, 1701–1710.
12 Koyuncu, F. B.; Koyuncu, S.; Ozdemir, E. *Electrochim. Acta* **2010**, 55, 4935–4941.
13 Liu, B.; Yu, W. L.; Lai, Y. H.; Huang, W. *Chem. Mater.* **2001**, 13, 1984–1991.
14 Kim, K. S.; Jeon, Y. M.; Kim, J. W.; Lee, C. W.; Gong, M. S. *Org. Electron.* **2008**, 9, 797–804.
15 Farcas, A.; Jarroux, N.; Harabagiu, V.; Guégan, P. *Eur. Polym. J.* **2009**, 45, 795–803.
16 Nie, G. M.; Yang, H. J.; Chen, J.; Bai, Z. M. *Org. Electron.* **2012**, 13, 2167–2176.
17 Qi, T.; Liu, Y.; Qiu, W.; Zhang, H.; Gao, X.; Liu, Y.; Lu, K.; Du, C.; Yu, G.; Zhu, D. *J. Mater. Chem.* **2008**, 18, 1131–1138.
18 Chowdury, M. A. H.; Monkman, A. P.; Chawdhury, N. *J. Polym. Res.* **2011**, 18, 1379–1384.
19 Bin, J. K.; Yang, J. H.; Hong, J. I. *J. Mater. Chem.* **2012**, 22, 21720−21726.
20 Han, C.; Zhang, Z.; Xu, H.; Yue, S.; Li, J.; Yan, P.; Deng, Z.; Zhao, Y.; Yan, P.; Liu, S. *J. Am. Chem. Soc.* **2012,** 134, 19179−19188.
21 Wang, L.; Wu, Z. Y.; Wong, W. Y.; Cheah, K. W.; Huang, H.; Chen, C. H. *Org. Electron.* **2011**, 12, 595−601.
22 Qiao, Y.; Wei, Z.; Risko, C.; Li, H.; Bredas, J. L.; Xu, W.; Zhu, D. *J. Mater. Chem.* **2012**, 22, 1313−1325.
23 Fortnagel, P.; Harms, H.; Wittich, R. M.; Francke, W.; Krohn, S.; Meyer, H. *Naturwissenschaften* **1989**, 76, 222–223.
24 Fortnagel, P.; Wittich, R. M.; Harms, H.; Schmidt, S.; Franke, S.; Sinnwell, V.; Wilkes, H.; Francke, W. *Naturwissenschaften* **1989**, 76, 523–524.
25 Monna, L.; Omori, T.; Kodama, T. *Appl. Environ. Microbiol.* **1993**, 59, 285–289.
26 Han, C.; Xie, G.; Xu, H.; Zhang, Z.; Yu, D.; Zhao, Y.; Yan, P.; Deng, Z.; Li, Q.; Liu, S. *Chem. Eur. J.* **2011**, 17, 445–452.
27 Han, C.; Zhao, Y.; Xu, H.; Chen, J.; Deng, Z.; Ma, D.; Li, Q.; Yan, P. *Chem. Eur. J.* **2011**, 17, 5800–5811.
28 Han, C.; Xie, G.; Xu, H.; Zhang, Z.; Xie, L.; Zhao, Y.; Liu, S.; Huang, W. *Adv. Mater.* **2011**, 23, 2491–2497.
29 K. W. Lin, S. J. Zhen, S. L. Ming, J. K. Xu, B. Y. Lu, *New J. Chem.* **2015**, 39, 2096–2105.
30 Camurlu, P.; Duraka, T.; Balan, A.; Toppare, L. *Synth. Met.,* **2011**, 161**,** 1898–1905.
31 Camurlu, P.; Duraka, T.; Toppare, L. *J. Electroanal. Chem.* **2011**, 661, 359–366.
32 Dong, S. C.; Zhang, L.; Liang, J.; Cui, L. S.; Jiang, Z. Q.; Liao, L. S. *J. Phys. Chem. C,* **2014**, 118, 2375–2384.
33 Jaramillo-Isaza, F.; Turner, M. L. *J. Mater. Chem.* **2006**, 16, 83–89.
34 Pang, Y. H.; Xu, H.; Li. X. Y. *Electrochem. Commun.* **2006**, 8, 1757–1761.
35 Thomas, S.; Zhang, C.; Sun, S. S. *J. Poly. Sci. A: Poly. Chem.* **2005**, 43, 4280–4289.
36 Shimomura, O.; Sato, T.; Tomita, I.; Suzuki, M.; Endo, T. *J. Polym. Sci. Part A Polym.Chem.* **1997**, 35, 2813–2819.
37 Turner, W. R.; Werbel, L. M. *J. Med. Chem.* **1985**, 28, 1728–1740.
38 Yang, W.; Hou, Q.; Liu, C.; Niu, Y.; Huang, J.; Yang, R.; Cao, Y. *J. Mater. Chem.* **2003**, 13, 1351–1355.
39 Steckler, T. T.; Henriksson, P.; Mollinger, S.; Lundin, A.; Salleo, A.; Andersson, M. R. *J. Am. Chem. Soc.* **2014**, 136, 1190–1193.
40 Cheng, Y. J.; Yang S. H.; Hsu, C. S. *Chem. Rev.* **2009**, 109, 5868–5923.
41 Sonmez, G. *Chem. Commun.* **2005**, 5251–5259.
42 Zhou, H.; Yang, L.; Price, S. C.; Knight, K. J.; You, W. *Angew. Chem. Int. Ed.* **2010**, 122, 8164–8167.

43 Piron, F.; Leriche, P.; Mabon, G.; Grosu, I.; Roncali, J. *Electrochem. Commun.* **2008**, 10, 1427−1430.

44 Nie, G. M.; Bai, Z. M.; Chen, J.; Yu, W. Y. *ACS Macro Lett.* **2012**, 1, 1304−1307.

45 Nie, G. M.; Yang, H. J.; Wang, S.; Li. X. M. *Crit. Rev. Solid State Mater. Sci.* **2011**, 36, 209–228.

46 Zhou, M.; Heinze, J. *Electrochim. Acta* **1999**, 44, 1733–1748

47 Lu, B. Y.; Zhen, S. J.; Zhang, S. M.; Xu, J. K.; Zhao, G. Q. *Polym. Chem.* **2014**, 5, 4896–4908.

48 Roncali, J.; Garnier, F. *Synth. Met.* **1986**, 15, 323–331.

49 Inzelt, G.; Pineri, M.; Schultze, J. W.; Vorotyntsev, M. A. *Electrochim. Acta* **2000**, 45, 2403–2421.

50 Vorotyntsev, M. A.; Badiali, J. P. *Electrochim. Acta* **1994**, 39, 289–306.

51 Inzelt, G.; Pineri, M.; Schultze, J. W.; Vorotyntsev, M. A. *Electrochim. Acta* **2000**, 45, 2403–2421.

52 Nie, G. M.; Bai, Z. M.; Yu, W. Y.; Chen, Juan. *Biomacromolecules* **2013,** 14, 834−840.

53 Uckert, F.; Tak, Y. H.; Müllen, K.; Bässler, H. *Adv. Mater.* **2000**, 12, 905–908.

54 Roncali, J.; Garnier, F. *Synth. Met.,* **1986**, 15, 323–331.

55 Xu, J. K.; Hou, J.; Zhang, S. S.; Nie, G. M.; Pu, S. Z.; Shen, L.; Xiao, Q. *J. Electroanal. Chem.* **2005**, 578, 345–355.

56 Dong, B.; Xing, Y. H.; Xu, J. K.; Zheng, L. Q.; Hou, J.; Zhao, F. *Electrochim. Acta* **2008**, 53, 5745–5751.

57 Lu, B. Y.; Yan, J.; Xu, J. K.; Zhou, S. Y.; Hu, X. J. *Macromolecules* **2010**, 43, 4599–4608.

58 Thieblemont, J. C.; Brun, A.; Marty, J.; Planche, M. F.; Calo, P. *Polymer,* **1995**, 36, 1605–1612.

59 Lim, B.; Nah, Y. C.; Hwang, J. T.; Ghim, J.; Vak, D.; Yuna, J. M.; Kim, D. Y. *J. Mater. Chem.* **2009**, 19, 2380–2385.

60 Unur, E.; Beaujuge, P. M.; Ellinger, S.; Jung, J. H.; Reynolds, J. R. *Chem. Mater.* **2009**, 21, 5145–5153.

61 Beaujuge P. M.; Reynolds, J. R. *Chem. Rev.* **2010**, 110, 268–320

62 Dyer, A. L.; Thompson, E. J.; Reynolds, J. R. *Appl. Mater. Interfaces* **2011**, 3, 1787–1795.

63 Ozkut, M. I.; Algi, M. P.; Oztaş, Z.; Algi, F.; Önal, A. M.; Cihaner, A. *Macromolecules* **2012**, 45, 729–734.

64 Güneş, A.; Cihaner, A.; Önal, A. M. *Electrochimica Acta* **2013**, 89, 339–345.

65 Çarbaş, B. B.; Kivrak, A.; Önal, A. M. *Electrochimica Acta* **2011**, 58, 223–230.

66 Data, P.; Zassowski, P.; Lapkowski, M.; Domagala, W.; Krompiec, S.; Flak, T.; Penkala, M.; Swist, A.; Soloducho, J.; Danikiewicz, W. *Electrochimica Acta* **2014**, 122, 118–129.

67 Hu, B.; Lv, X. J.; Sun, J. W.; Bian, G. F.; Ouyang, M.; Fu, Z.Y.; Wang, P. J.; Zhang, C. *Org. Electron.* **2013**, 14, 1521–1530.

68 Koyuncu, F. B.; Koyuncu, S.; Ozdemir, E. *Org. Electron.* **2011**, 12, 1701–1710.

69 Nie, G. M.; Zhou, L. J.; Yang, H. J. *J. Mater. Chem.* **2011**, 21, 13873–13880.

Graphic for manuscript:

Molecular design of DBT/DBF hybrid thiophenes π-conjugated systems and comparative study on their electropolymerization and optoelectronic properties: from monomers to electrochromic polymers

Kaiwen Lin, Shouli Ming, Shijie Zhen, Yao Zhao, Baoyang Lu* and Jingkun Xu*

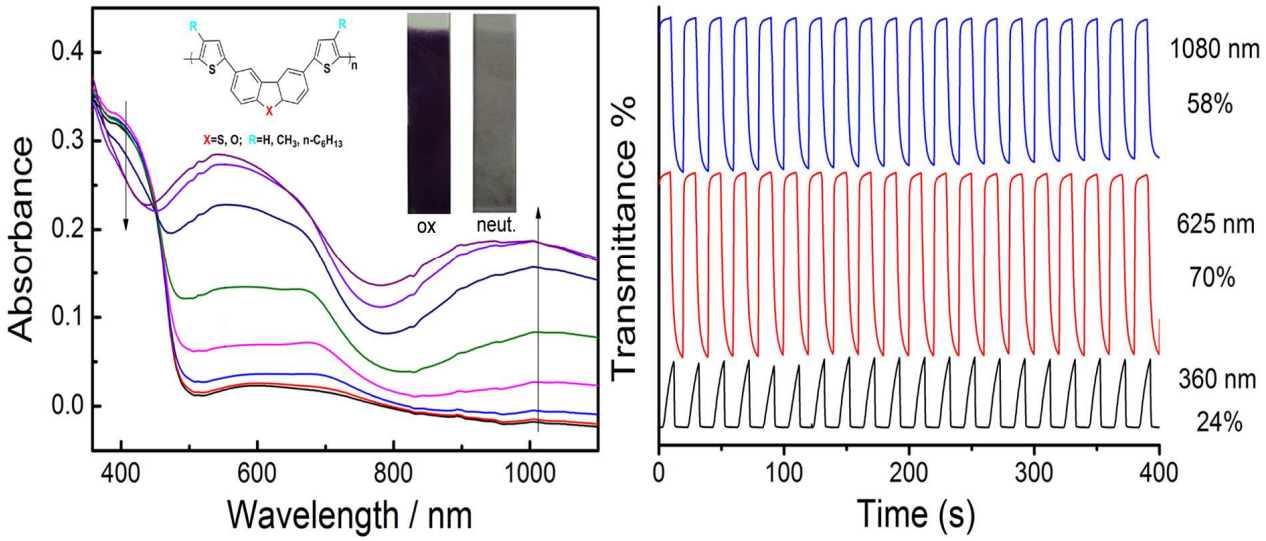

A series of DBT/DBF end-capped with thiophenes comonomers were designed and electropolymerized to yield novel electrochromic polymers with good performances.